Chapter 13

Examples of IOP Applications

Robert Arnone, Hubert Loisel, Kendall Carder, Emmanuel Boss, Stephane Maritorena and ZhongPing Lee

The IOPs retrieved from ocean colour provide innovative tools and opportunities for oceanographic studies, as their values can be used directly or indirectly to study biological and biogeochemical processes in the oceans (Gould and Arnone, 1997; Bissett *et al.*, 2001; Coble *et al.*, 2004; Hu *et al.*, 2004, 2005). For instance, earlier studies (Kirk, 1984; Sathyendranath and Platt, 1988) have shown that the diffuse attenuation coefficients of the water can be adequately estimated from water's inherent optical properties. Recent studies (Stramski *et al.*, 1999; Loisel *et al.*, 2001a; Balch *et al.*, 2005) have shown that particulate carbon can be well estimated from particle backscattering coefficient. Further, a new generation of biological models (Bissett *et al.*, 2005; Penta *et al.*, 2005) now integrate explicitly two or more species of plankton, as well as dissolved (DOC) and particulate organic carbon (POC), whereas IOPs play important roles in observing and monitoring blooms of red tides (Cullen *et al.*, 1997; Cannizzaro *et al.*, 2006). As confidence in the IOP products continues to grow, our understanding of how IOP properties are linked to ocean processes expands. This research is moving the ocean community beyond the traditional applications centered on the oceanic chlorophyll-a. In this chapter, we present some examples of IOP applications in this regard.

13.1 Water Composition and Water-Mass Classification

The absorption and backscattering coefficients bring some complementary information on the water composition, because of their different sensitivity to the various optically significant materials in water. While the absorption coefficient is affected by the presence of both suspended and dissolved material in water, the backscattering coefficient represents the concentration (to first order) of organic and inorganic suspended particles, and bubbles. The decomposition of the total absorption coefficient into its different components, as discussed in Chapter 1, allows the monitoring of phytoplankton and of the remaining absorbing

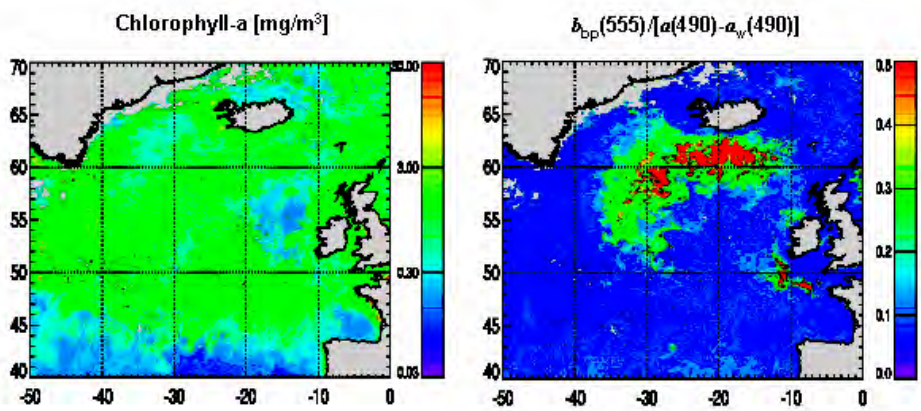

Figure 13.1 Comparison between the SeaWiFS-chlorophyll concentration and the ratio of the particle backscattering to absorption obtained from an inverse algorithm (Loisel and Stramski, 2000) over the North Atlantic (south Island) in June 1998. As seen, C and $b_{bp}(555)/(a(490)\text{-}a_w(490))$ represent different patterns, with the latter clearly showing different particle populations. These particles have been identified as coccolithophorid, which are characterized by a high backscattering efficiency.

materials. Therefore, synoptic satellite observations of a and b_b give a valuable picture of composition of surface waters. For example, the b_{bp}/a ratio may be used to discriminate different families of particles (Figure 13.1).

New applications have also used the IOP characteristics of the water as a tool to fingerprint a water mass and identify the controlling optical processes (Traykovski and Sosik, 2003; Arnone and Parsons, 2004). Besides water absorption, the total absorption is additionally composed of the absorption from CDOM, detritus and phytoplankton (see Chapter 1). By defining the percent contribution of each of these components, a water mass can be defined by which component controls the absorption budget. A ternary plot of these three components provides a useful method for fingerprinting water mass and the dominant absorption process (Gould and Arnone, 2003; Arnone *et al.*, 2004). This method has been applied to satellite absorption properties derived from semi-analytical algorithms for SeaWiFS and MODIS ocean-colour imagery (Figure 13.2a). This water-mass classification can be represented by an RGB image representing percent detritus, phytoplankton and CDOM absorption (Figure 13.2b). These images easily illustrate the controlling biogeochemical processes for monitoring coastal and offshore water masses. Note that this classification method identifies the dominance of the absorption processes, and not the absolute values of the absorption coefficients. This classification method can be used on sequential satellite images of the absorption components to identify changes in absorption processes and to track water masses based on a specific fingerprint of the absorption components.

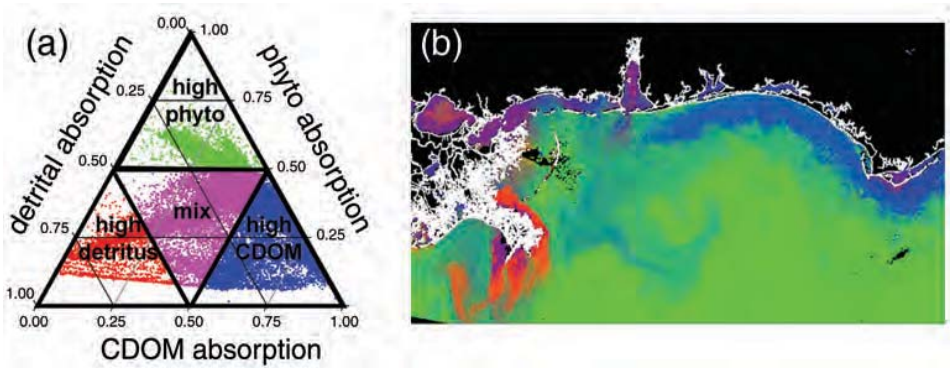

Figure 13.2 (a) Water-mass classification from the absorption budget. Ternary plot of the percent absorption attributed to detritus, CDOM and phytoplankton for each pixel to identify the dominant components. (b) RGB image of percent absorption of detritus (red), phytoplankton (green) and CDOM (blue). Absorption products derived from SeaWiFS were used to determine the absorption budget. Intensity of the colour indicates the dominant component

13.2 Dissolved and Particulate Organic Carbon

Examination of the temporal variations of absorption and backscattering coefficients and comparison with that of chlorophyll over the global ocean have also provided important information about the dynamics of marine particles and dissolved organic carbon, because the absorption and backscattering coefficients are related to different biogeochemical parameters. For instance, the feasibility of estimating POC (in mg m^{-3}), and the coloured detrital and dissolved materials (CDM) (in m^{-1}), from the remotely detected b_b and a was recently demonstrated (Stramski *et al.*, 1999; Loisel *et al.*, 2001b; Loisel *et al.*, 2002; Siegel *et al.*, 2002; Balch *et al.*, 2005) (see Figures 13.3 and 13.4). A phase shift between the annual cycles of b_{bp} and chlorophyll was evidenced, and was attributed to the presence of a pool of non-pigmented particles originating from the accumulation of dead phytoplankton cells, as well as zooplankton detritus, in the summer stratified surface layer (Loisel *et al.*, 2002). The decrease of the Chl/POC ratio in living phytoplankton at high irradiance in summer was also used to explain the lag between the Chl and b_{bp} maxima (Loisel *et al.*, 2002).

Figure 13.4 shows global distributions of CDM of two seasons in 1998, derived from SeaWiFS data (Siegel *et al.*, 2002). Clearly, there are significant spatial and temporal variations in global CDM (a part of DOC). Because POC and CDM represent different pools of carbon stored in oceans, and since CDM plays an important role in regulating subsurface blue/ultraviolet radiation (Siegel *et al.*, 2002), analysis of their spatial/temporal distributions is important for the understanding of the carbon cycles in oceans.

Behrenfeld *et al.* (2005), using backscattering and chlorophyll-a derived from

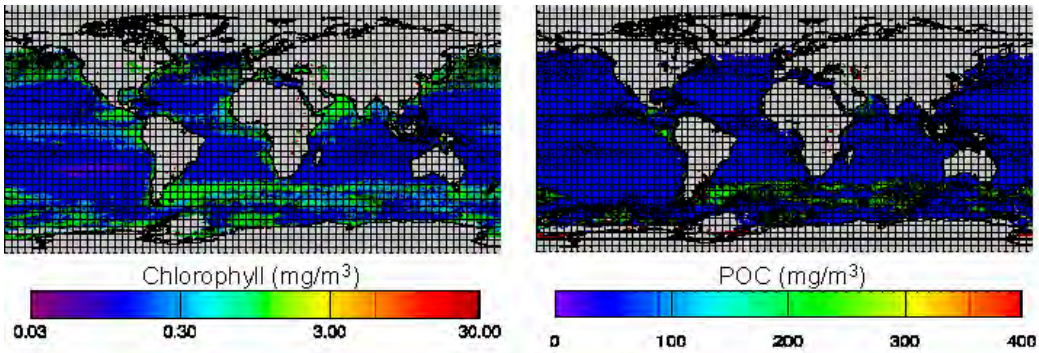

Figure 13.3 Global chlorophyll (SeaWiFS product) and POC distribution in January 2000 (adapted from Loisel *et al.*, 2002).

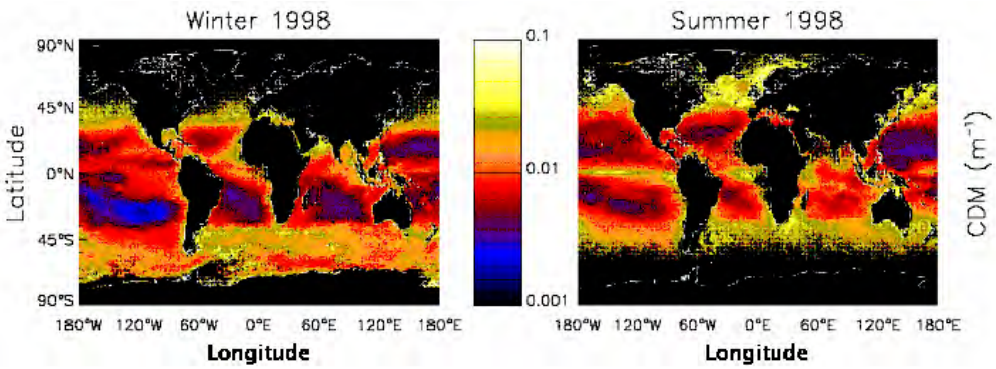

Figure 13.4 Global distribution of CDM (in m^{-1}) derived from SeaWiFS data by the GSM algorithm (Chapter 11) (adapted from Siegel *et al.*, 2002).

R_{rs} as inputs, also developed a novel primary production model based on the physiological link between phytoplankton growth rate and growth conditions (temperature, nutrients, and light) as reflected in the ratio of chlorophyll to carbon of phytoplankton. This novel (and debatable) approach is to use the backscattering coefficient to estimate phytoplankton biomass and assuming a linear relation between total POC and phytoplankton biomass. The observed change (Figure 13.5) in the ratio of chlorophyll-a to phytoplankton carbon is interpreted as reflecting a physiological change, rather than a change in the particulate composition. Net primary production is then computed from the estimated growth rate through a simple multiplication by the phytoplankton carbon and a function that accounts for its vertical distribution with depth.

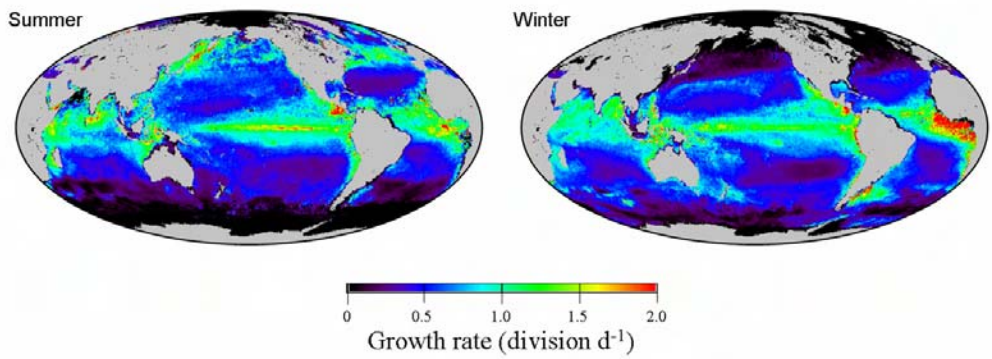

Figure 13.5 Phytoplankton growth rates for Boreal summer (June to August) and winter (December to February). Adapted from Behrenfeld *et al.* (2005).

13.3 Diffuse Attenuation Coefficient of Downwelling Irradiance

The availability of absorption (a) and backscattering coefficients (b_b) also makes it straightforward to calculate the diffuse attenuation coefficient of downwelling irradiance, either at a single wavelength ($K_d(\lambda)$) or for the broad band (350 - 700 nm) visible domain (K_{vis}). Because both K_d and K_{vis} are apparent optical properties, they are directly linked to the IOPs (Sathyendranath and Platt, 1988; Gordon, 1989; Lee *et al.*, 2005a,b). Traditionally, estimation of K_d is based on the spectral ratios of $L_w(\lambda)$ or $R_{rs}(\lambda)$. Such an approach does not reveal the fundamental relationship between AOPs and IOPs, and is found to work only for waters with limited dynamic range (Mueller, 2000). Figure 13.6(a) shows a comparison between measured $K_d(490)$ and R_{rs} derived $K_d(490)$, for a wide range of $K_d(490)$ (0.04 - 4.0 m^{-1}) measured from different regions and at different times, using an algorithm based on a and b_b whose values were derived first from R_{rs} (Lee *et al.*, 2005b). Clearly, excellent agreement is achieved between the two independent measurements and determinations.

K_{vis} (wavelength range of 350 - 700 nm) is a parameter needed for models of oceanic photosynthesis and heat transfer in the upper water column. K_{vis} varies significantly from the surface to depth (z), even for vertically homogeneous waters, which is different from the characteristics of K_d. To represent this vertical variation, earlier studies used multiple exponential terms to describe the vertical propagation of visible solar radiation, with the coefficients of these multiple terms expressed as empirical functions of chlorophyll (Morel and Antoine, 1994; Ohlmann and Siegel, 2000). Again, realizing the intrinsic limitations between an optical property (*e.g.*, K_{vis}) and chlorophyll, a model has been developed (Lee *et al.*, 2005a) that can be used to adequately estimate the vertical variation of K_{vis}

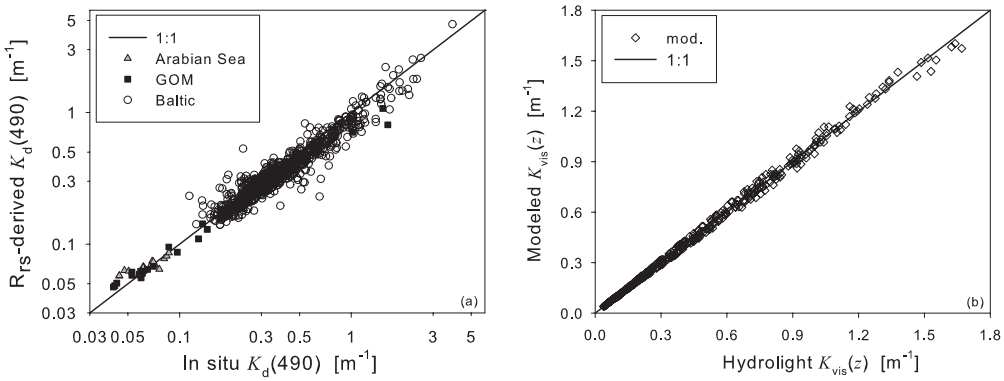

Figure 13.6 (a) Measured $K_d(490)$ vs R_{rs}-derived $K_d(490)$. In the derivation of K_d from R_{rs}, values of a and b_b were derived from R_{rs} first, and then K_d is calculated based on these a and b_b values (from Lee *et al.*, 2005b). (b) modelled $K_{vis}(z)$ compared with $K_{vis}(z)$ from Hydrolight simulations (adapted from Lee *et al.*, 2005a).

when values of $a(490)$ and $b_b(490)$ are available. Figure 13.6(b) shows modelled K_{vis} compared with Hydrolight-calculated K_{vis} for different values of a, b_b, and z. The average difference between the two sets of $K_{vis}(z)$ is 2.2%.

13.4 Oceanic Primary Production

Knowing the values of IOPs can also provide some basic information for the estimation of oceanic primary production. Currently, this estimation is done centred on the values of chlorophyll-a concentration (Platt and Sathyendranath, 1988; Behrenfeld and Falkowski, 1997). When chlorophyll is used as an input parameter representing the function of phytoplankton, a value regarding the chlorophyll-specific absorption coefficient is also explicitly or implicitly utilized. Numerous field measurements (Bricaud *et al.*, 1995; Cleveland, 1995; Lutz *et al.*, 1996; Bricaud *et al.*, 1998) and theoretical studies (Bricaud and Morel, 1986) have pointed out that this property varies widely from place to place and time to time, therefore large uncertainties are automatically introduced when this parameter is involved. Because primary production measures the conversion of solar energy absorbed by phytoplankton to sustenance in the photosynthetic process (Morel, 1978; Smith *et al.*, 1989), remotely derived or locally measured phytoplankton absorption and other IOPs can then be utilized directly in this estimation (Zaneveld *et al.*, 1993). One example of taking this approach is demonstrated in Lee *et al.* (1996a), with Figure 13.7 showing primary production calculated from values of R_{rs} (along with other auxiliary information) compared with primary production measured from *in situ* incubation.

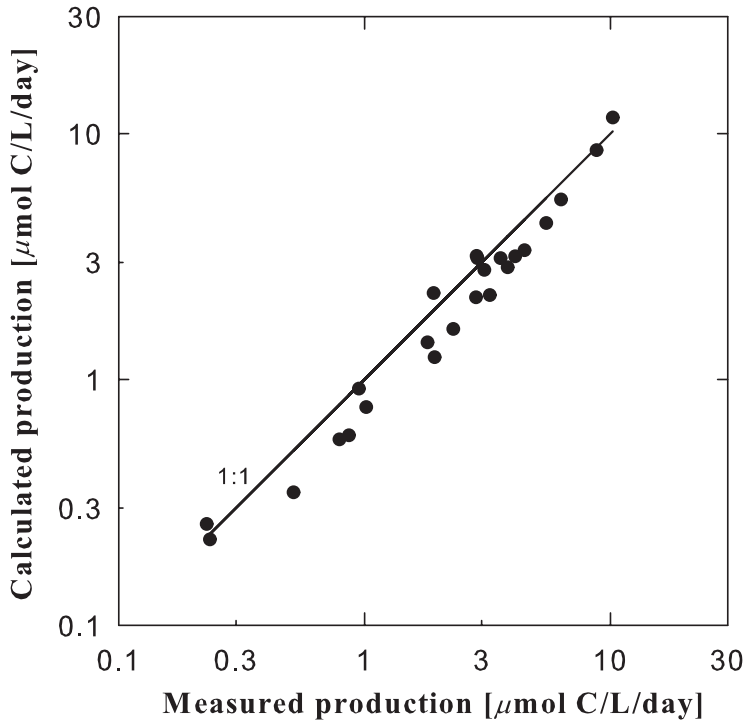

Figure 13.7 Daily primary production calculated from R_{rs} versus that from *in situ* incubation. Adapted from Lee *et al.* (1996a)

13.5 Chlorophyll Concentration from Remotely Derived Pigment Absorption Coefficient

When the absorption coefficient of phytoplankton pigment is derived from ocean colour, it adds the possibility of deriving the concentration of chlorophyll-a (Carder *et al.*, 1999; Lyon *et al.*, 2004) for different regions of the world, as indicated in Carder *et al.* (1999). Applying the semi-analytic code (Carder *et al.*, 1999) to an upwelling site (Smyth *et al.*, 2002) and a river-plume site (Hu *et al.*, 2003), it provided much more realistic estimations of chlorophyll concentration for both cases (where the empirical band-ratio approach (OC4) underestimated the high chlorophyll concentrations of the upwelling site and overestimated chlorophyll concentration for gelbstoff-rich river-plume regions). MODIS-Terra chlorophyll images from the GES DAAC (Goddard Earth Science Distributed Active Archive Center) derived by the semi-analytic code (chl_a_3) and empirical-ratio code (chl_a_2) were composited in 39-km bins for December 2000 and are shown in Figure 13.8. The subtropical gyre regions appear similar for the two images, but the chlorophyll values are clearly elevated with the semi-analytic code for the high-latitude and equatorial upwelling regions which have higher pigment concentrations.

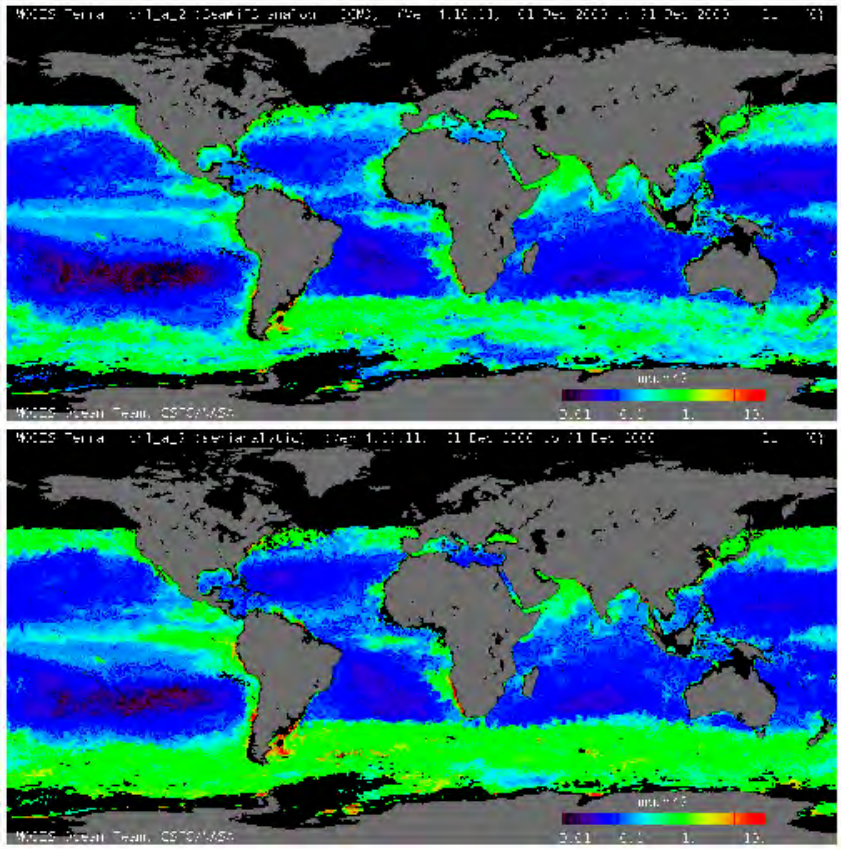

Figure 13.8 Global composited maps (December 2000) of chlorophyll-a concentration (mg m^{-3}) retrieved using empirical (top) and semi-analytic (bottom) algorithms from MODIS-Terra radiometry (adapted from Carder *et al.*, 2004).

13.6 Monitoring Coastal Ocean Processes using IOPs and Numerical Circulation Models

IOPs provide an improved capability to understand how physical processes influence the bio-optical processes (Bissett *et al.*, 2001; Arnone and Parsons, 2004). For instance, ocean colour IOP products from MODIS and SeaWiFS are being integrated with numerical circulation models. The Navy Coastal Ocean Model (NCOM) is forced by large scale ocean models which currently assimilate sea surface height from altimetry and sea surface temperature (SST) from AVHRR. These models are at 32-degree resolution with 41 sigma levels to characterize the mesoscale features (`http://www7320.nrlssc.navy.mil/global_ncom/`). Overlaying the modelled properties (currents, salinity, surface heights) with optical properties adds continuity to understanding IOP image products. This fusion of physical models and IOP imagery enables improved understanding of the distri-

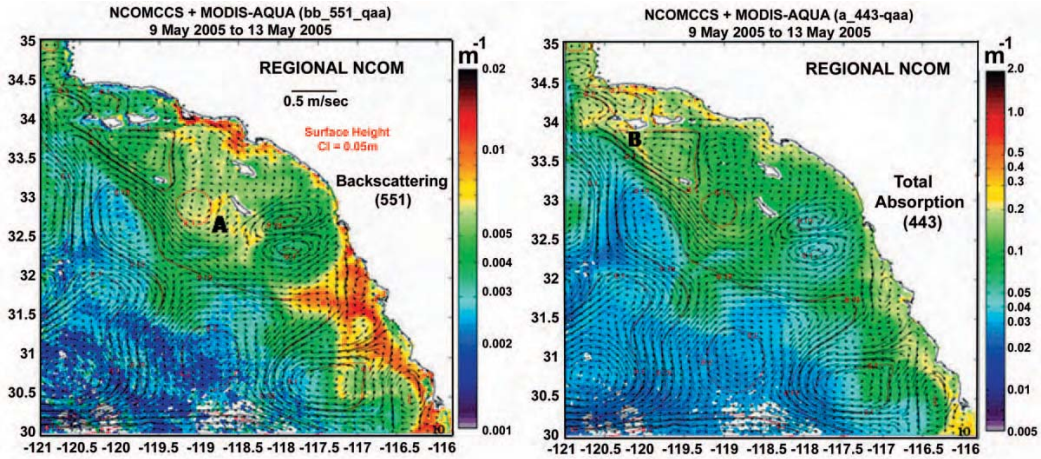

Figure 13.9 The circulation along the California Coast develops coastal filaments shown in surface currents and MODIS-Aqua IOP products. Differences in the locations of backscattering at 551 nm (associated with particles) and the total absorption at 443 nm (detritus, CDOM and phytoplankton) indicate varying bio-optical processes within these filaments.

bution of bio-optical processes that are linked with mesoscale ocean circulation features. Different IOP properties, such as backscattering, CDOM and phytoplankton absorption respond differently to mesoscale processes. Along the U.S. West coast, filaments associated with the California Current System are driven by the physical circulation as shown in Figure 13.9 (Shulman *et al.*, 2004; Penta *et al.*, 2005). The corresponding IOP distribution within these filaments is used to define the response of bio-optical processes. For example, the influence of the strong southerly flow off the Channel Islands is characterized by backscattering and total absorption products. Within this filament, the elevated particles are located south of the strong flow (point A) as shown in the $b_b(551)$ image (a result of advection), whereas the strongest currents (point B) located close to land have elevated total absorption as shown in the $a(443)$ image (a result of coastal upwelling). Divergent and convergent mesoscale fronts are revealed by the IOP properties observed in satellite imagery (Figure 13.9). Similar differences in the distribution of backscattering and absorption have been observed by Otero and Siegel (1995).

13.7 Conclusions

Our understanding of how the optical properties of water constituents are related to ocean processes has advanced significantly in the last decade. Use of IOPs to characterize ocean processes provides improved methods for monitoring and understanding the role of the oceans on a global scale. Because IOPs are

closely associated with the water leaving radiance measured by satellites and IOP retrievals are robust and stable as shown in previous chapters, IOP products are critical for monitoring and detecting changes in the ocean's climatology and forecasting ocean biogeochemical processes.